Radio and optical properties of extragalactic radio sources with recurrent jet activity

Marek Jamrozy

Obserwatorium Astronomiczne Uniwersytetu Jagiellońskiego

Energetics and life-cycles of radio sources

ASTRON, 26-28 March 2018

A. P. Schoenmakers,
A. G. de Bruyn,
H. J. A. Rottgering,
H. van der Laan,
C. R. Kaiser
2000, MNRAS, 315, 371

WENSS 326 MHz
Rengelink et al.
1997, A&AS, 124, 259

B0925+420

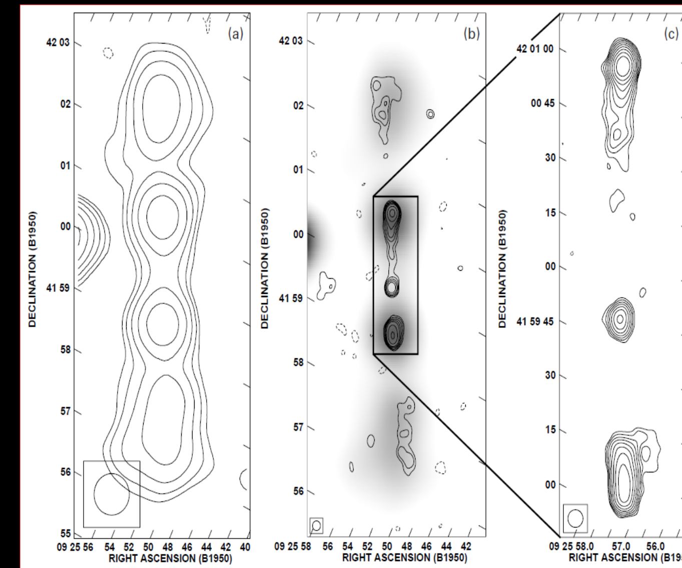

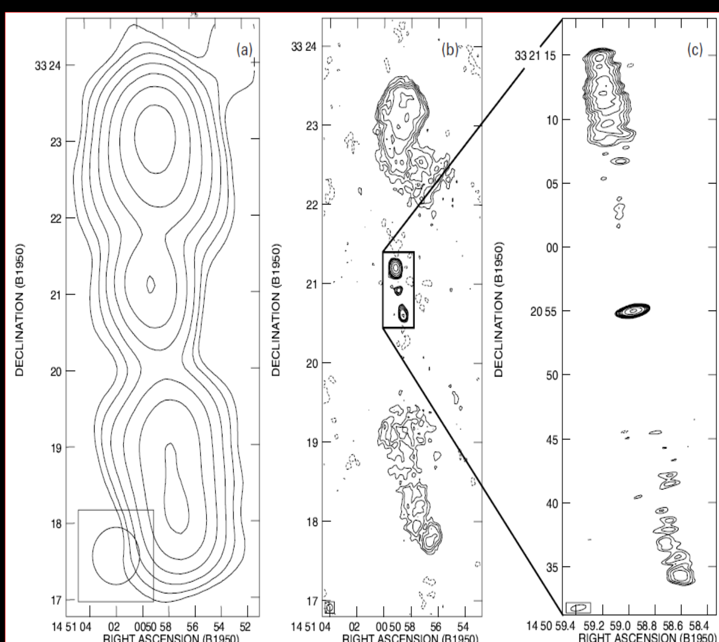

B1450+333

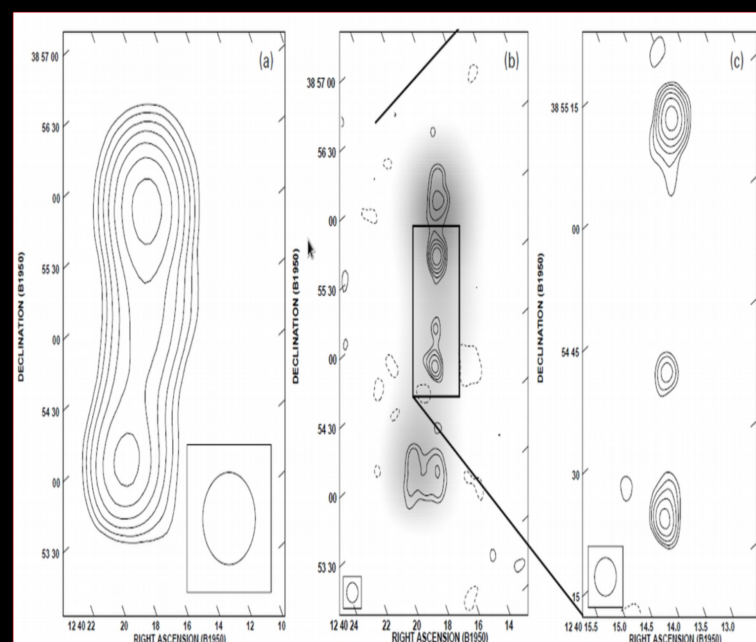

B1240+389

DDRG – two unequall sized , two sided, double lobed, edge-brightened (FRII) radio sources from two different cycles
of activity.

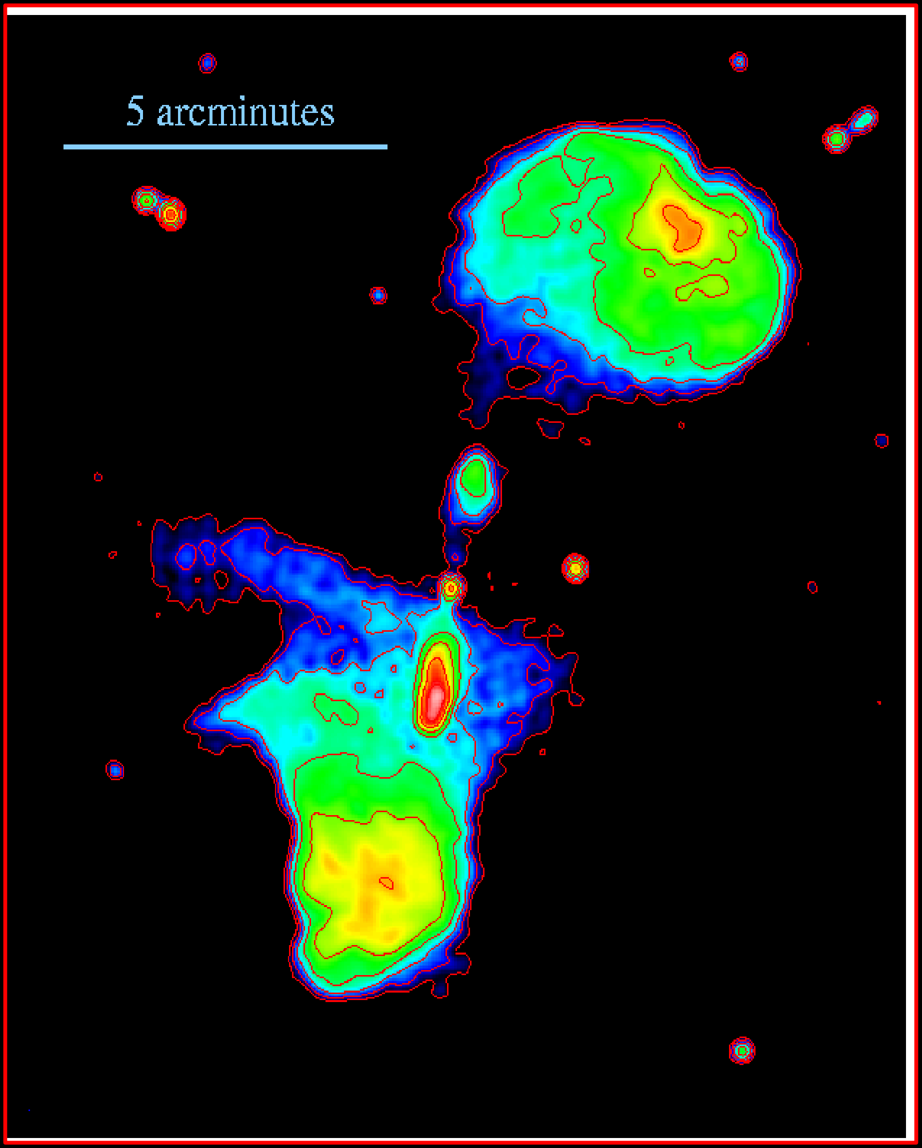

Saripalli, Subrahmanyan, Udaya Shankar, 2003, ApJ, 590, 181

Easy to recognise

Morphological characteristics of restarters

- No hotspots in outer lobes
- Large axial-ratio of inner lobes
- Inverse spectrum or variable core

Interruptions related to:

→ refueling of the central engine

→ instabilities in the accretion disk

→ jet production machanism

Difficult to recognize

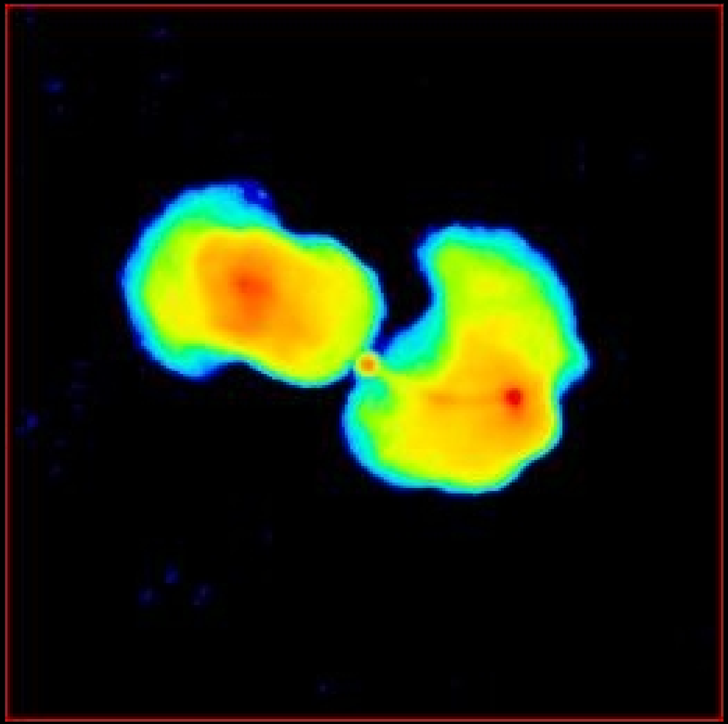

3C388 z=0.0917 size=1'

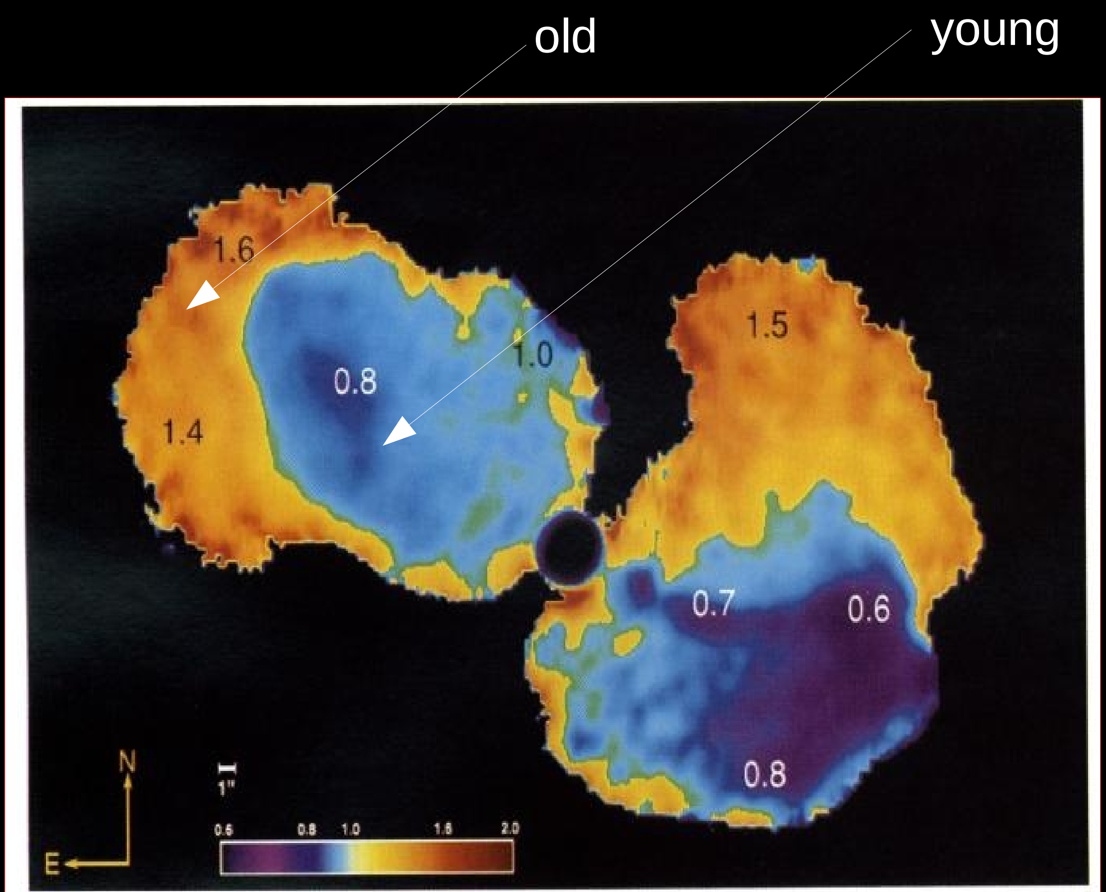

FIG. 2.—Spectral index (4.847–1.385 GHz) map of 3C 388. Several regions are labeled with typical spectral index values.

Roettiger, Burns, Clarke, & Christiansen, 1994, ApJ, 421, L23

Relic radio emission in 3C388

Abstract

New VLA images of the radio galaxy **3C 388 have revealed an intriguing distribution** of spectral indices which is **quite different from that of typical classical double sources**. We observe two distinct regions of emission separated by a well-defined transition layer delineated by a dramatic jump in the spectral index, particularly in the eastern lobe. We interpret these data as **evidence of at least two distinct epochs of jet activity** in which the current jets have resumed penetration of the IGM and are inflating younger, more energetic lobes into the relic lobes of the previous epoch. To the best of our knowledge, 3C 388 is the **first radio galaxy in which multiple epochs of activity** are clearly visible in the large-scale radio structure.

J0349+7511 (Abell 449) z = 0.08

ultra-steep spectrum 1.3 Mpc giant

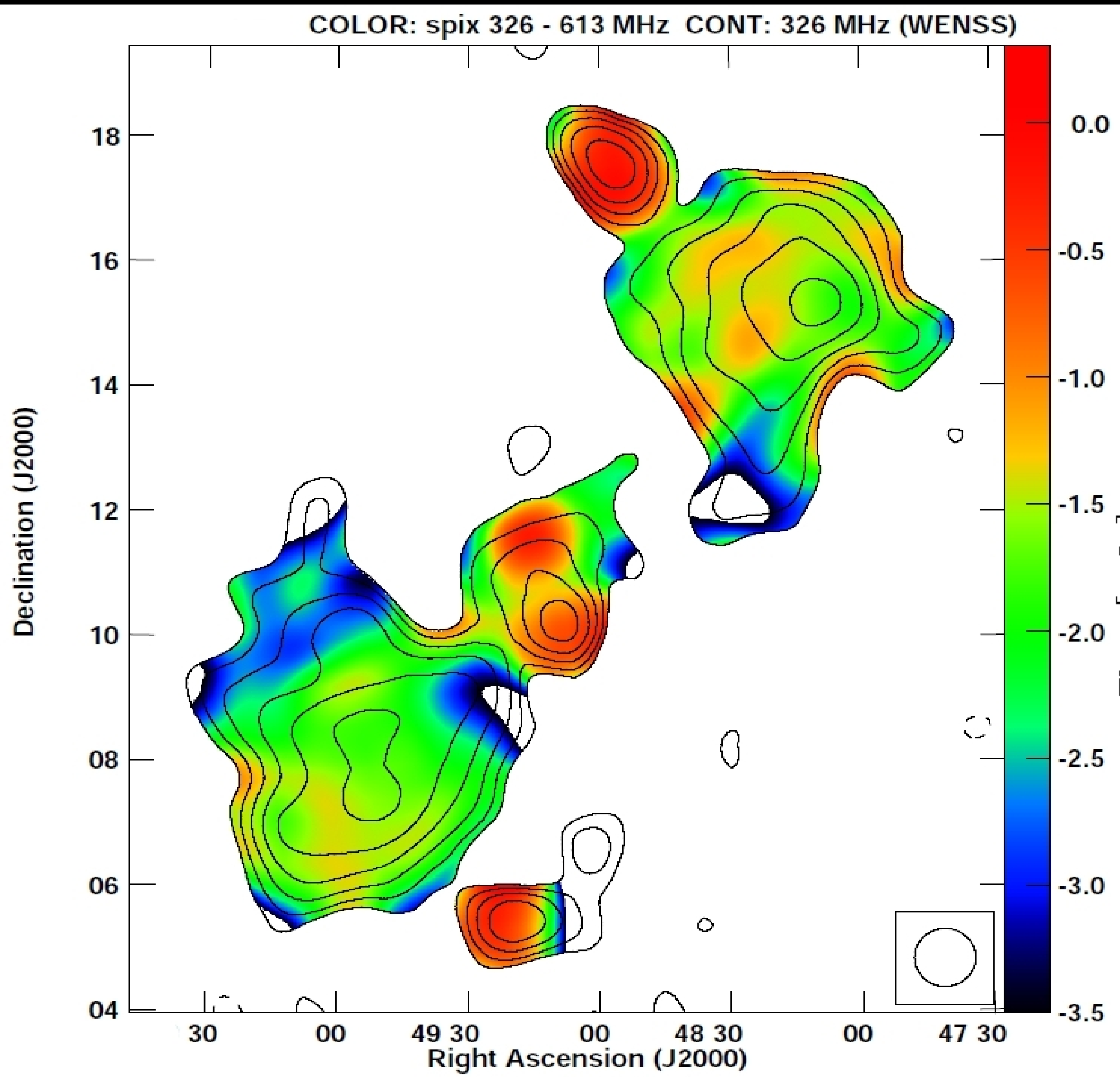

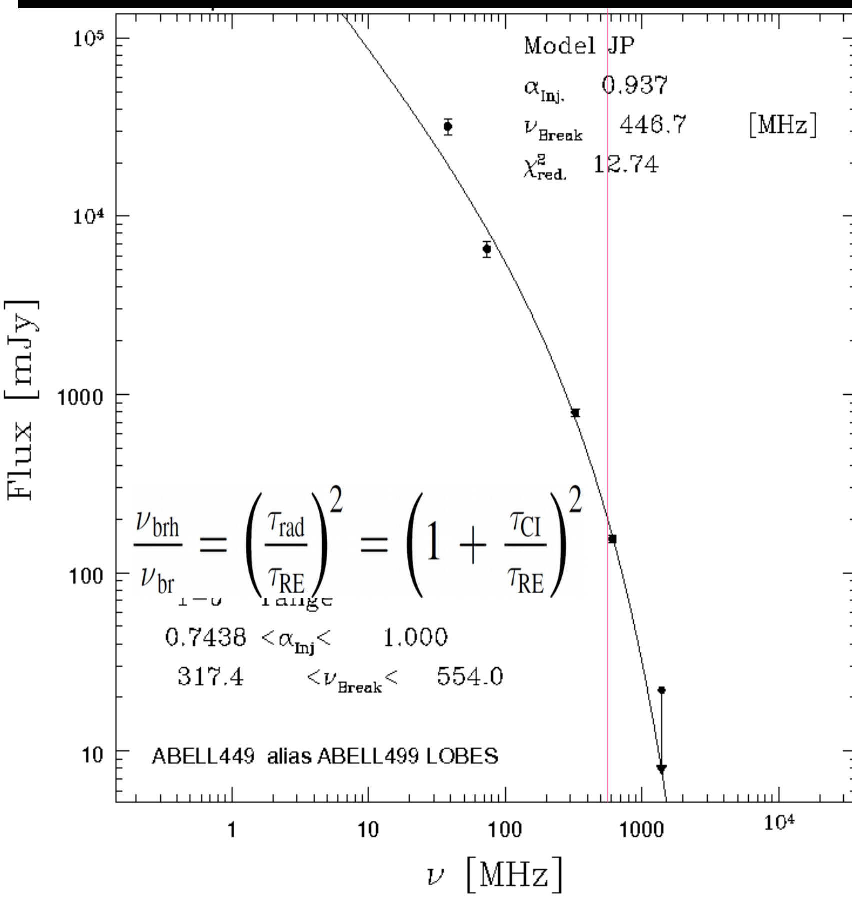

Hunik & Jamrozy, 2016, ApJL, 817, 1

mean synchrotron age of the lobes' particles is about **160±20Myr** (ν_{br} =450 ±120 MHz)

J0349+7511

Ghost at high radio frequencies

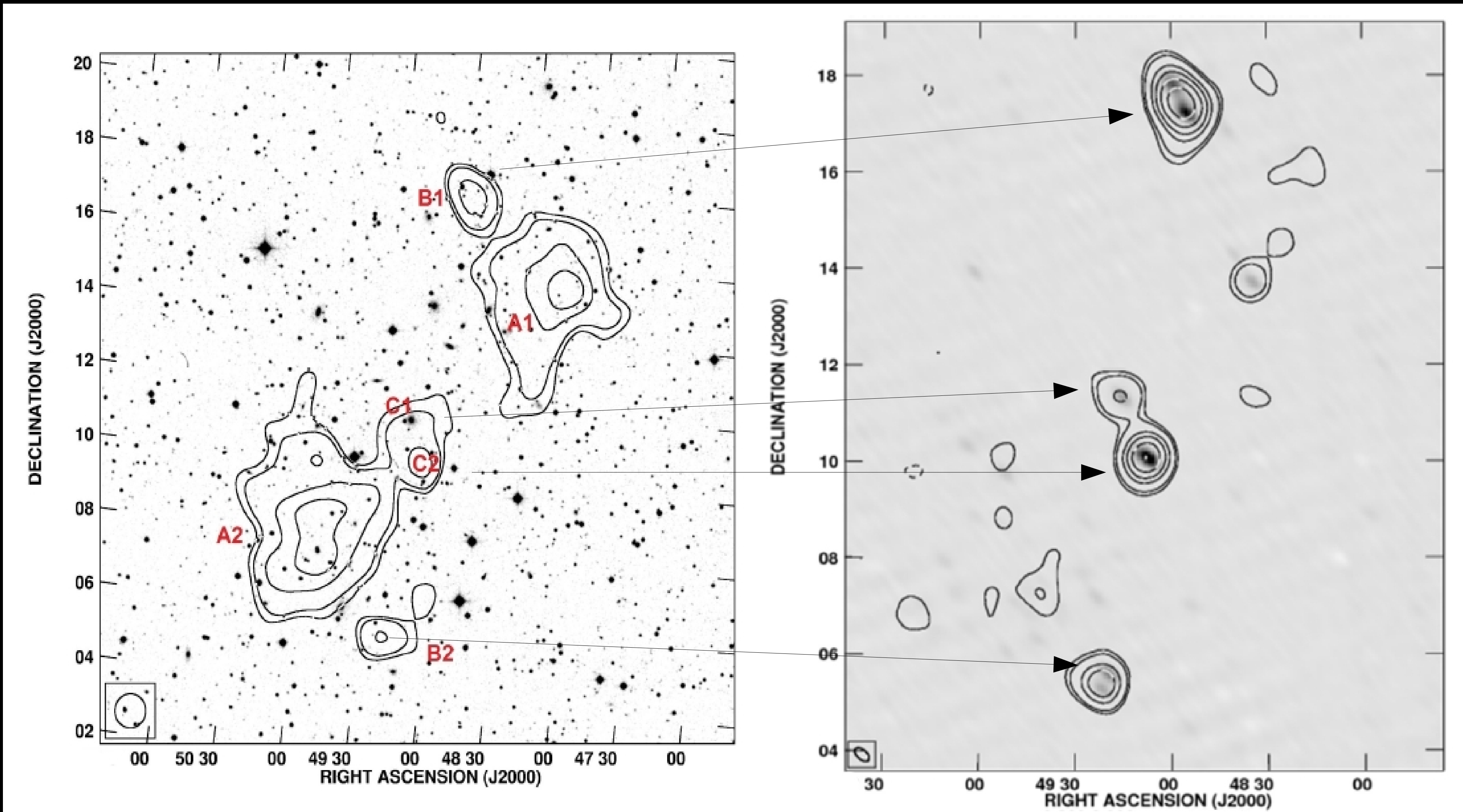

WENSS

NVSS

Weak cocoons

4C 29.30

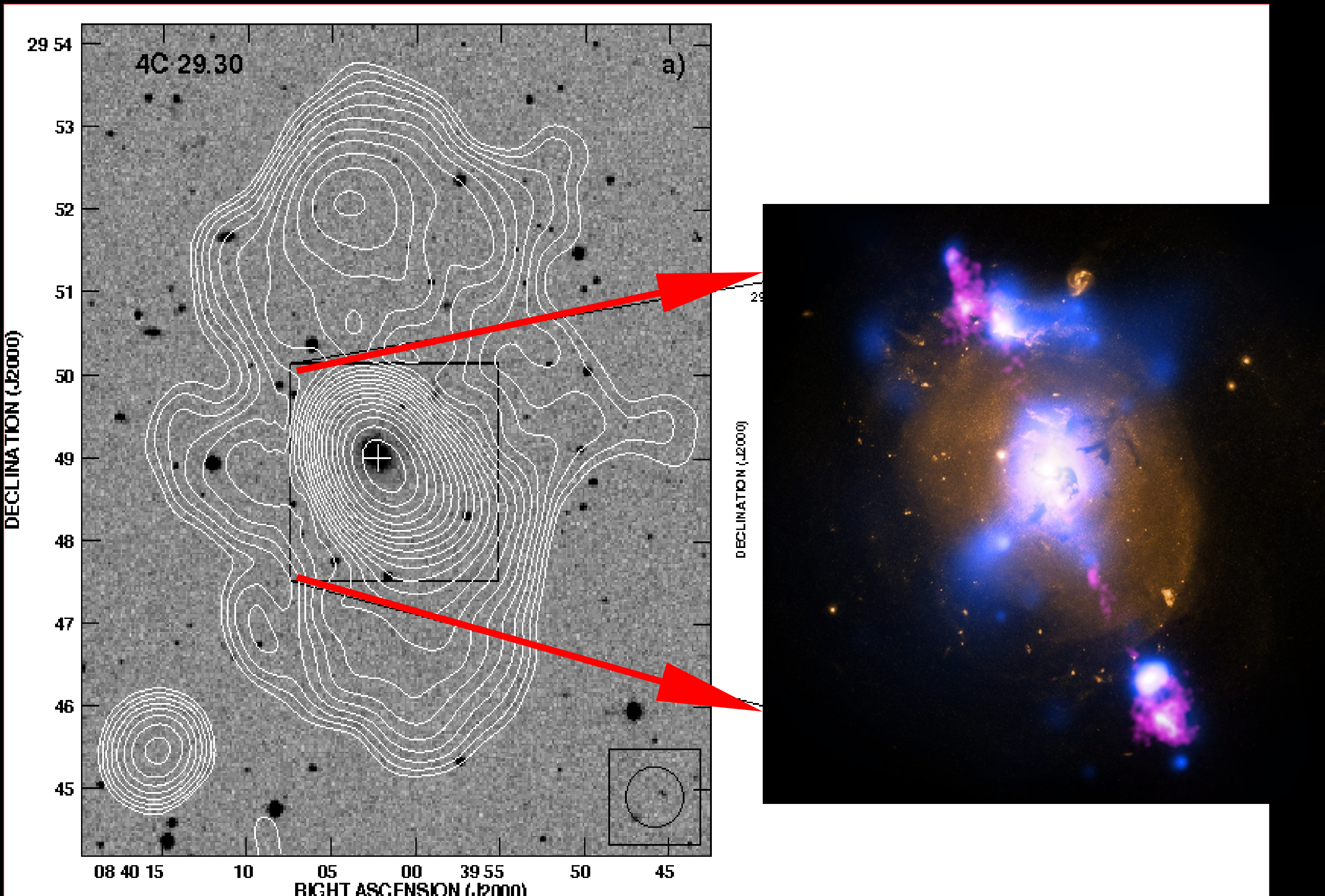

Jamrozy et al., 2007, MNRAS, 378, 581

Siemiginowska, et al. 2012, ApJ, 750, 124

Radio sources with recurrent jet activity

- 74 sources
- 67 galaxies, 2 quasars
- 0.002 < z < 0.7
- 0.02 < D < 4284 kpc

Kuzmicz et al., 2017, MNRAS, 471, 3806

Table 1. Radio sources with evidence of recurrent activity.

Source (name) (1)	IAU (name) (2)	$RA_{J2000.0}$ (h m s) (3)	$Dec._{J2000.0}$ (° ′ ″) (4)	Opt. (Id.) (5)	Red-(shift) (6)	l_{in} (kpc) (7)	l_{in} (arcsec) (8)	l_{out} (kpc) (9)	l_{out} (arcsec) (10)	S_{in} (mJy) (11)	S_{out} (mJy) (12)	$\log M_{BH}$ ($M_\odot$) (13)	Class (A/B) (14)	Ref. (Cmt.) (15)
J0009+1244	4C12.03	00 09 52.60	+12 44 04.64	G	0.156	114.9	43	553.1	207	100	907	–	A	1,f
J0037+1319	3C16	00 37 44.57	+13 19 55.00	G	0.405	96.91	18	419.9	78	35	1765	–	A	1,2
J0041+3224*		00 41 46.12	+32 24 52.65	G	(0.45)	172	30	974	170	525	409	–	A	3
J0042−0613		00 42 46.85	−06 13 52.92	G	0.123	518.1	237.1	753.6	344.9	690	1140	9.23	A	4,a,e
J0104−6609		01 04 21.26	−66 09 17.30	G	(1.19)	66.7	8	750	90	0.37	5.22	–	A	5
J0111+3906*	B0108+388	01 11 37.32	+39 06 28.10	G	0.6685	0.07	0.01	126.1	18	519	8	–	B?	6,b,c
J0116−4722		01 16 25.04	−47 22 41.60	G	0.146	455	180	1441	570	260	2640	–	A	7
J0301+3512*	4C 34.09	03 01 42.37	+35 12 20.68	G	0.0165	0.66	2	233.7	706	1800	119	8.26	B	2,i
J0301+3550*	4C 35.06	03 01 51.50	+35 50 30.00	G	0.0463	32.29	36	403.7	450	492	258	–	A	8
J0303+1626	3C76.1	03 03 15.02	+16 26 19.06	G	0.0325	21.8	34.1	107.1	167.4	450.2	2602	–	B	1
J0351−2744	PKS0349−27	03 51 35.76	−27 44 34.70	G	0.0662	251.8	200.8	437.8	349.1	2636	3009	–	A	9
J0504+3806	3C134	05 04 42.19	+38 06 11.40	G	–	–	115.6	–	166.1	1485	7862	–	A	a
J0709−3601	PKS0707−35	07 09 14.09	−36 01 21.80	G	0.218	627.1	179.4	1720	492	480	1444	–	A	10,11
J0741+3112*	B2 0738+31	07 41 10.70	+31 12 00.22	Q	0.632	0.03	0.005	478.5	70	2188	38	9.37	A	12,b,h
J0746+4526		07 46 17.92	+45 26 34.46	G	0.5502	95	15.2	640	100.1	24.2	191.6	9.96	A	13
J0804+5809		08 04 42.79	+58 09 34.94	S	–	–	21.6	–	106.3	58.6	192.1	–	A	13
J0821+2117*	B0818+214	08 21 07.50	+21 17 02.87	G	0.418	2.7	0.5	209.8	38.24	148	46.4	–	A	14
J0840+2949*	4C29.30	08 40 02.36	+29 49 02.63	G	0.0647	39.3	32	533.3	434.6	446.7	216.9	8.32	B	15
J0847+3147	IC2402	08 47 59.04	+31 47 08.37	G	0.0674	203	159.3	362.1	284.2	173.9	1303	9.28	A	16
J0855+4204		08 55 49.15	+42 04 20.11	G	(0.279)	35.3	8.4	545.9	130	18.8	155.7	–	A	13
J0910+0345*		09 10 59.10	+03 45 31.68	G	(0.588)	42.3	6.4	218.8	33.1	50.7	53.4	–	A	13
J0914+1006*		09 14 19.53	+10 06 40.59	G	0.308	216.2	48	1709	379.7	252.5	129.1	8.56	A	a
J0921+4538	3C219	09 21 08.61	+45 38 57.36	G	0.174	70.1	24	438.5	150	90	8046	8.43	A	17,18,19
J0924+0602		09 24 49.04	+06 02 42.80	G	0.231	80.8	22.1	424	116	4.8	90	8.85	A	a
J0927+2932		09 27 44.88	+29 32 32.30	S	–	–	24	–	115	19	17	–	A	8
J0927+3510		09 27 50.59	+35 10 50.73	G	(0.55)	575.5	90	2206	345	3	96	–	A	20
J0929+4146		09 29 10.66	+41 46 45.59	G	0.365	655.6	130	1876	372	64	99	–	A	21,d,g
J0935+0204	4C02.27	09 35 18.19	+02 04 15.54	Q	0.6491	69.9	10.1	498	71.96	230.3	547.6	9.56	A	22
J0943−0819[a]	B0941−080	09 43 36.94	−08 19 30.81	G	0.228	0.18	0.05	72.34	20	3232	26	–	B?	23,h
J1004+5434		10 04 51.83	+54 34 04.29	G	0.047	55.2	60.6	694.2	762.9	90	110	8.72	A	24,a
J1006+3454	3C236	10 06 01.73	+34 54 10.52	G	0.101	1.8	1	4248	2310	2500	3300	8.70	A	25,26,27
J1021+1216[a]		10 21 24.21	+12 17 05.44	G	0.129	876.4	385	1865	819.4	67.3	55	8.56	A	4,a
J1039+0536		10 39 28.21	+05 36 13.62	G	0.35	81.5	16.6	488.7	99.6	54.9	594.9	–	A	13
J1103+0636		11 03 13.29	+06 36 16.00	G	0.4406	66.3	11.7	548.8	96.9	13.2	79.9	8.24	A	13
J1158+2621	4C26.35	11 58 20.13	+26 21 12.07	G	0.112	139	69	483.8	240	67	962	7.96	A	13,28
J1159+5820		11 59 05.68	+58 20 35.57	G	0.054	23.2	22.4	348.2	335.8	5.3	319.1	8.60	A	29
J1208+0821		12 08 56.78	+08 21 38.57	G	0.5841	111.3	16.9	648.9	98.5	2	51.9	9.27	A	13
J1238+1602		12 38 21.20	+16 02 41.42	S	–	–	40.8	–	115.6	8.9	56.5	–	A	13
J1242+3838		12 42 36.82	+38 38 06.15	G	0.408	308.3	57	735.5	136	8	24	8.72	A	30
J1247+6723*		12 47 33.31	+67 23 16.46	G	0.107	0.019	0.01	1196	618	260	126	8.63	A	31,32
J1325−4301	Cen A	13 25 27.62	−43 01 08.81	G	0.0018	21.3	67	266.4[j]	1800[j]	$28\cdot 10^4$	$52\cdot 10^4$	–	A	33,34
								533	14 400		$96\cdot 10^4$			
J1326+1924		13 26 13.67	+19 24 23.75	G	0.1762	26	8.8	150.6	51	6	81.8	8.93	A	13
J1328+2752		13 28 48.45	+27 52 27.81	G	0.0911	97.3	58	220.8	131.7	27.9	219.9	7.82	A	13
J1344−0030		13 44 46.92	−00 30 09.31	G	0.5801	85.4	13	631	96.1	20.1	48.7	8.73	A	13
J1352+3126	3C293	13 52 17.88	+31 26 46.49	G	0.045	1.1	1.2	179.5	204.2	3703	1209	8.15	A	35
J1407+5132	4C51.31	14 07 18.48	+51 32 04.63	G	(0.324)	84.8	18.2	707.5	151.8	9.2	646.2	–	A	13
J1409−0302		14 09 48.85	−03 02 32.53	G	0.1378	52.9	22	308	128	4	48	8.61	A	36,d
								1373	570		112			
J1443+5201	3C303	14 43 02.75	+52 01 37.23	G	0.1412	81.9	33.3	90.9	37	1500	935	8.07	B	1
J1453+3308	4C33.33	14 53 02.86	+33 08 42.40	G	0.249	158.5	41	1299	336	34	426	9.02	A	30,37
J1500+1542		15 00 55.18	+15 42 40.56	G	(0.456)	124.2	21.5	480.7	83.2	11.1	17.8	–	A	13
J1504+2600	3C310	15 04 57.12	+26 00 58.46	G	0.0538	152.1	147.1	255.4	247	1547	5846	8.29	B	38

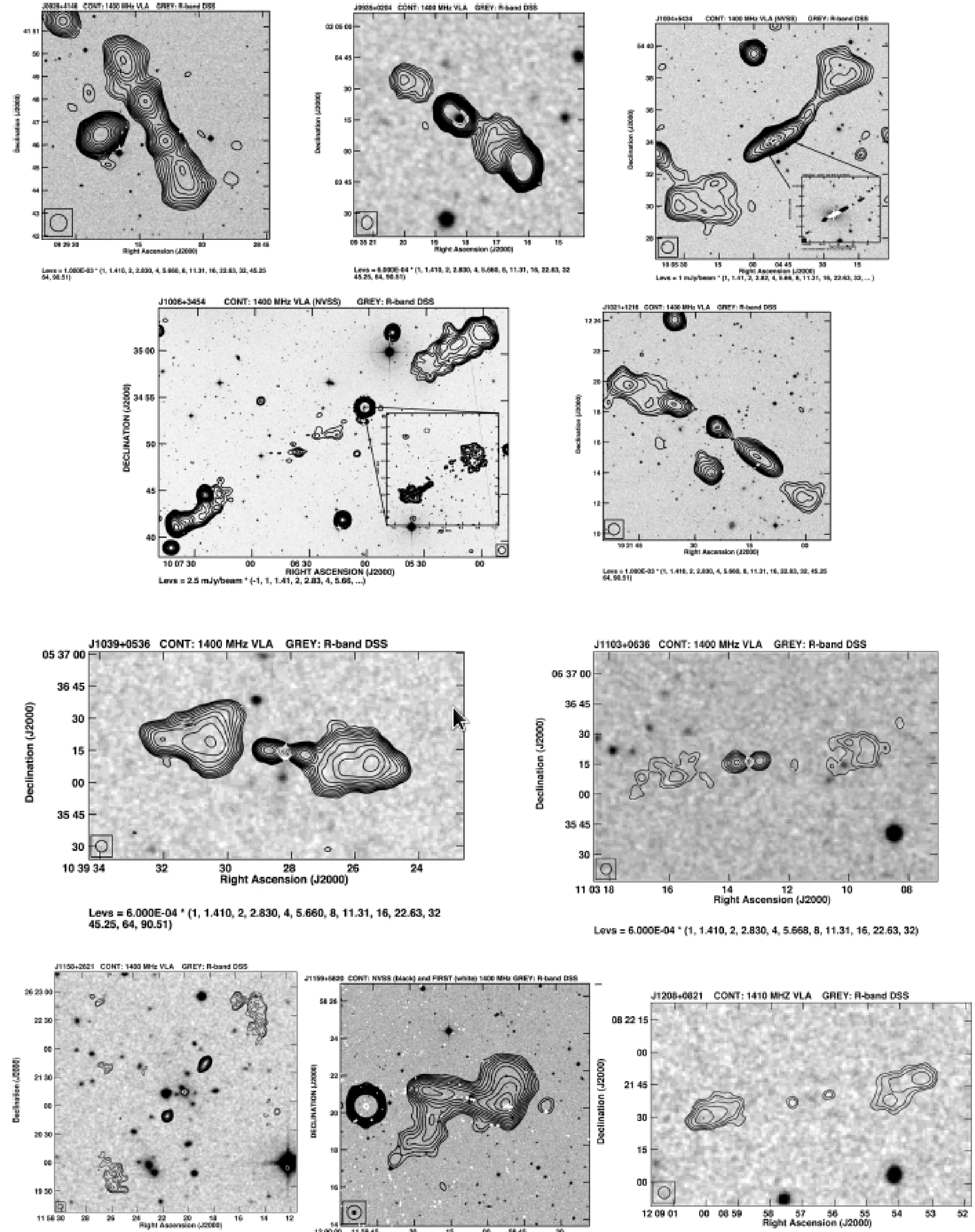

Kuzmicz et al., 2017,
MNRAS, 471, 3806

J1247+6723

Marecki et al. 2003,PASA, 20, 16

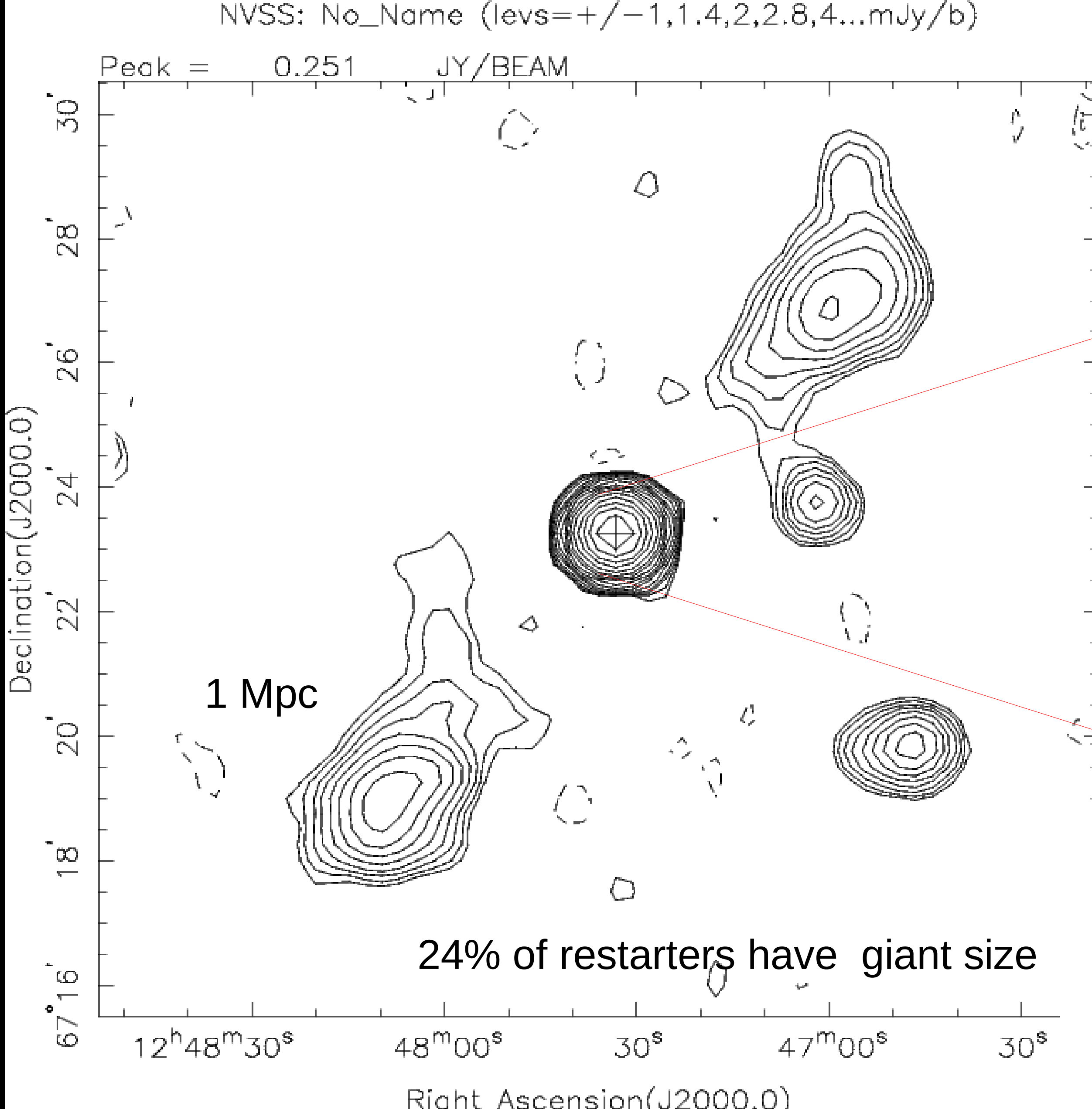

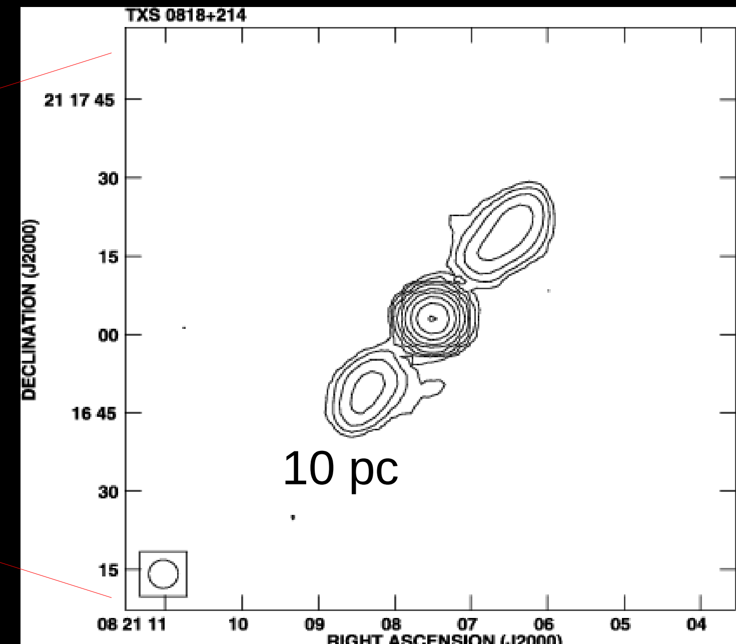

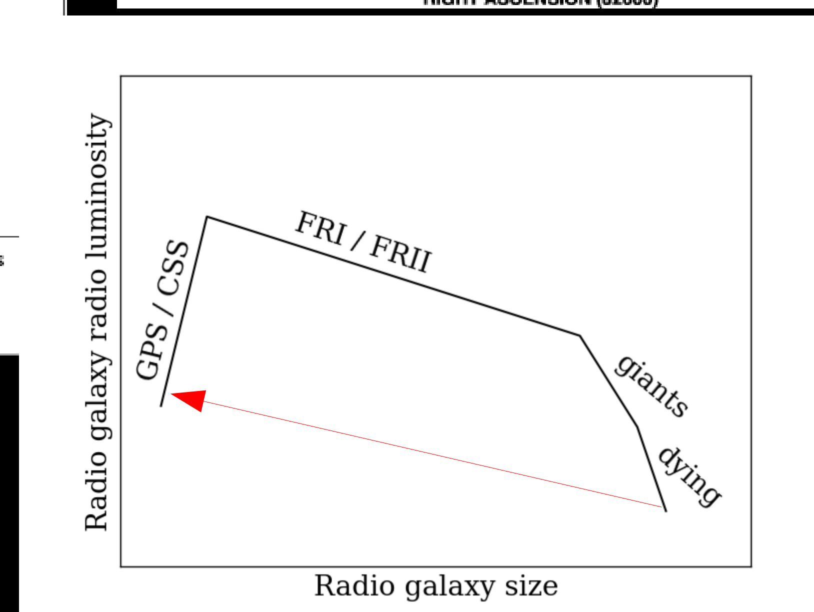

variable radio cores

Konar, Hardcastle, 2013, MNRAS, 436, 1595

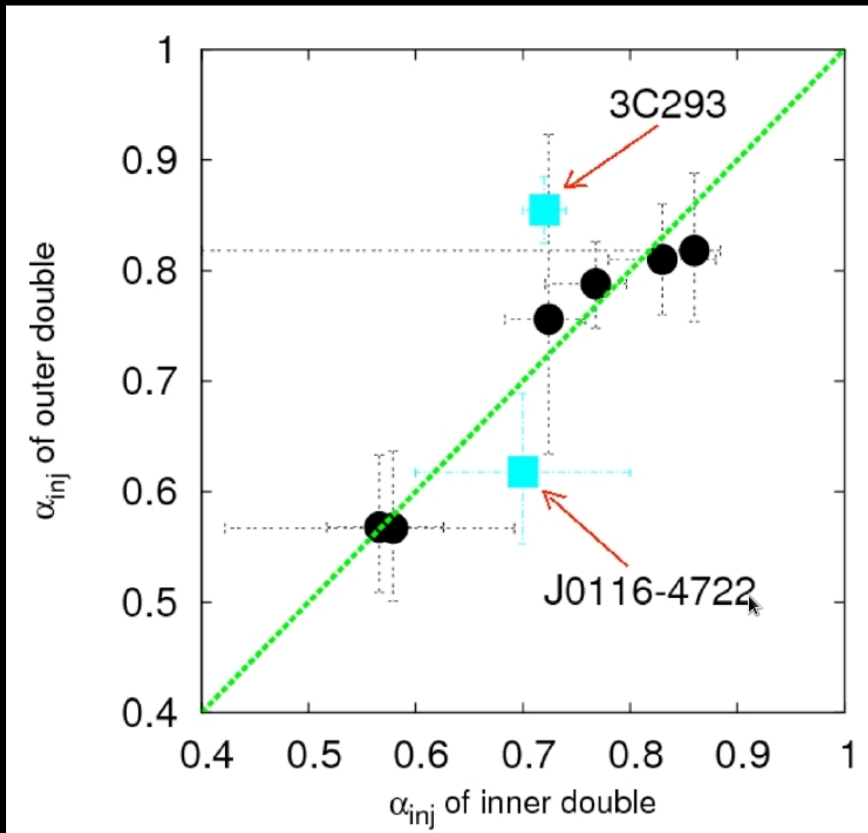

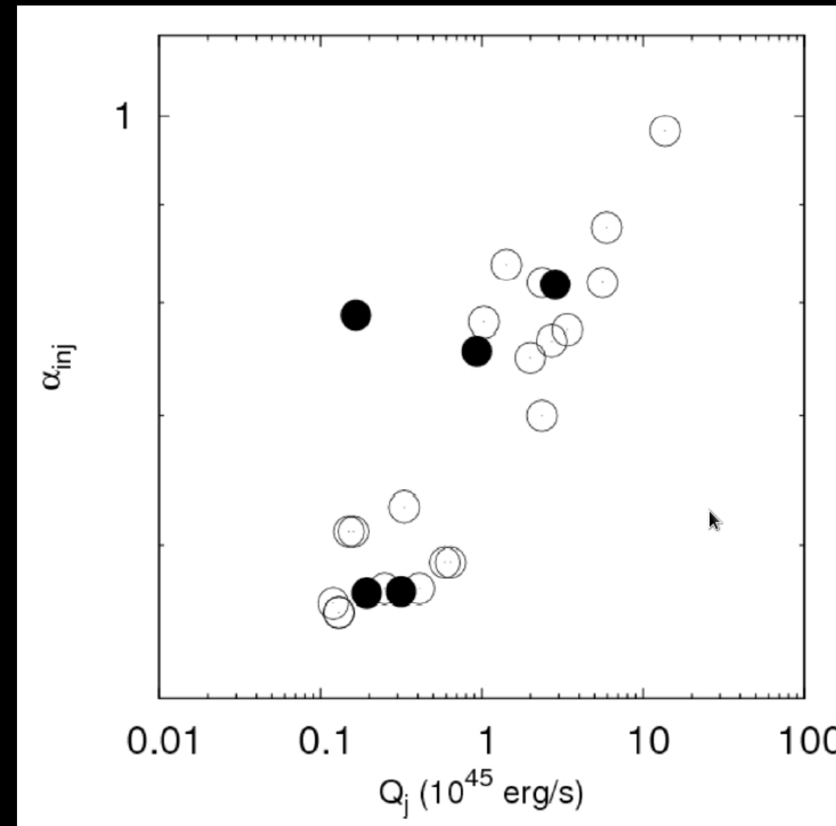

values of **injection index** (the low frequency power-law index of synchrotron emission) **are similar in the two different episodes** for most of the DDRGs

injection index is strongly dependent on the jet power

jet power in the two episodes of a DDRG needs to be the same, or at least similar,

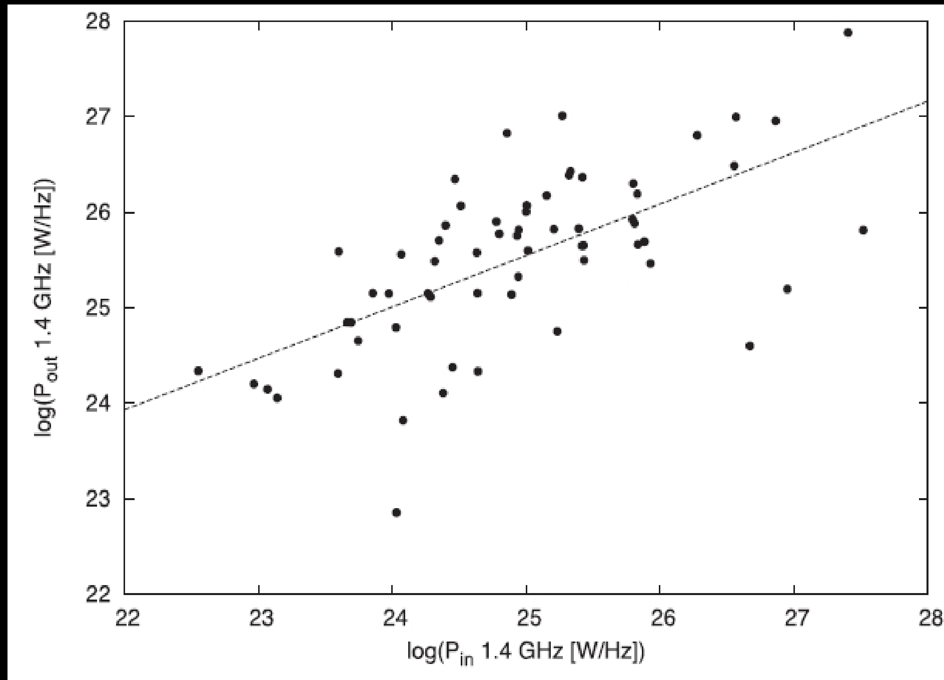

There is a strong correlation between the radio luminosity of the inner and outer lobes.

Source J2000 name (1)	Alt. name (2)	z (3)	Size (kpc) (4)	t_{quies} (Myr) (10)
J0041+3224	B2 0039+32	0.45	969	0.7–5.7
J0116−4722	PKS 0114−47	0.146 101	1447	1.4–65.4
J0840+2949	4C 29.30	0.064 715	639	2.0–102.0
J1158+2621	4C +26.35	0.112 075	483	6.6–11.0
J1453+3308	4C +33.33	0.248 174	1297	12.4–21.1
J1548−3216	PKS 1545−321	0.1082	961	0.05†–29.2
J1835+6204	B 1834+620	0.5194	1379	1.0–6.6
J1211+7419	4CT 74.17.01	0.1070	845	0.01–0.83$^{\xi}$

quiesence time ~10% age of the old structure

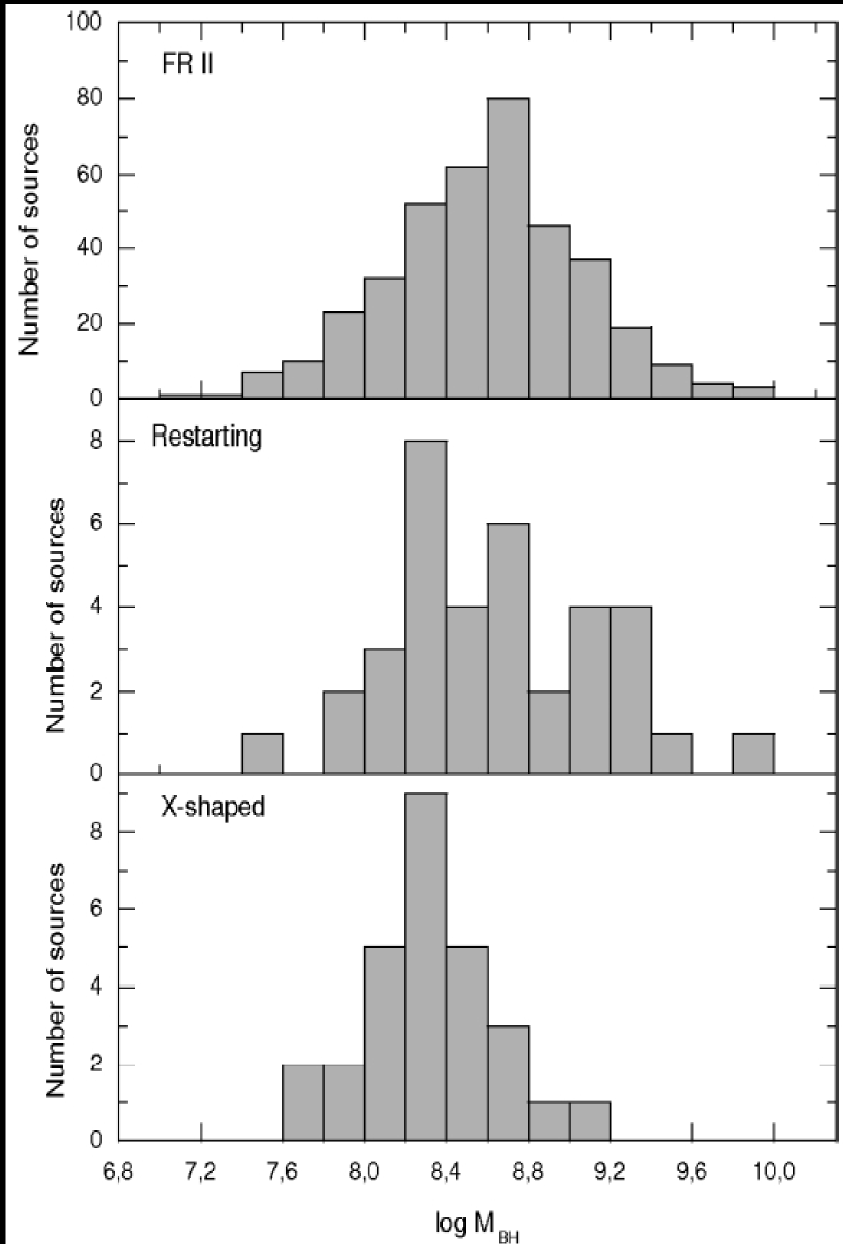

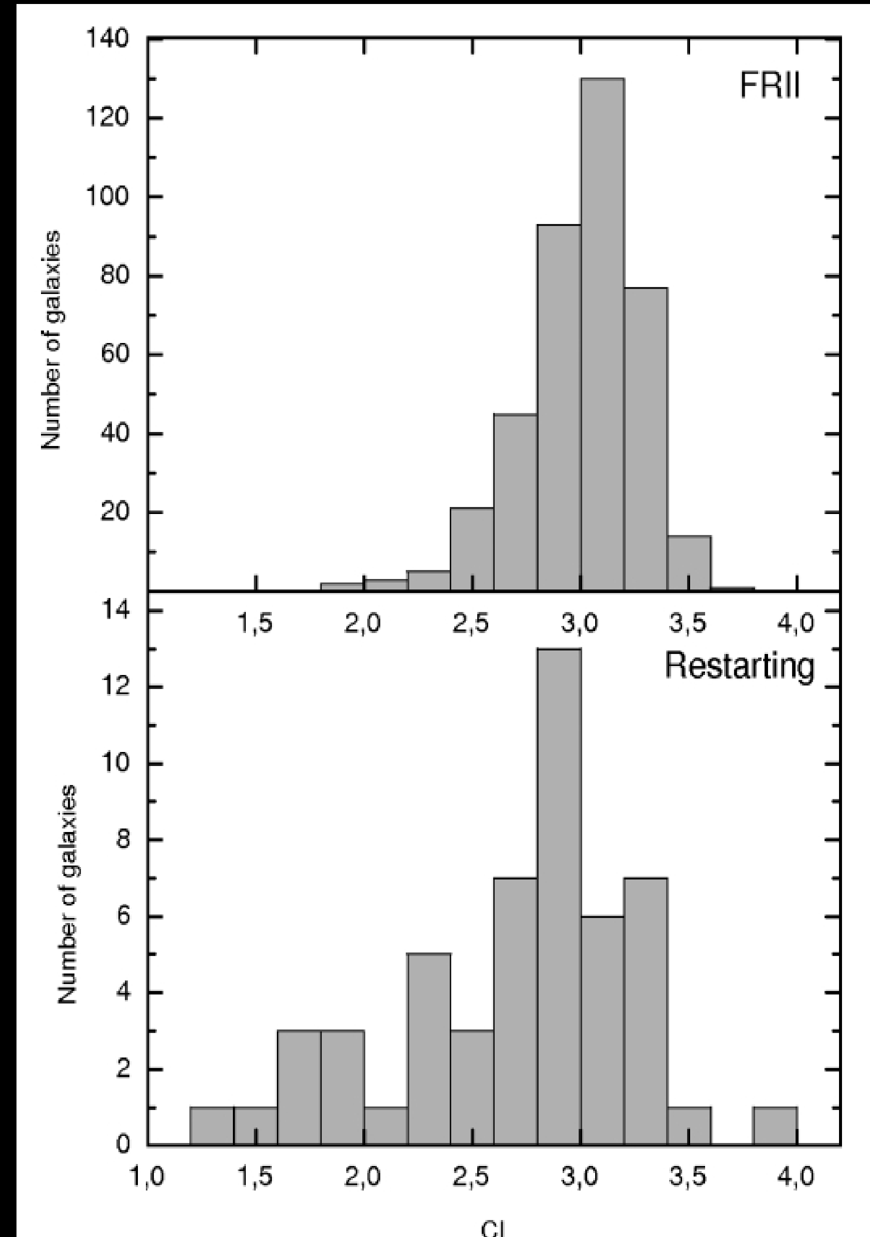

The BH masses of radio sources with recurrent activity are similar to those observed in FRII radio galaxies, median values of log MBH are 8.58 and 8.62 M_{SUN}

The CI for the restarting radio sources tends to be slightly lower than that of the FRII sources, which indicates that they can have **hosts with more disturbed morphologies**.

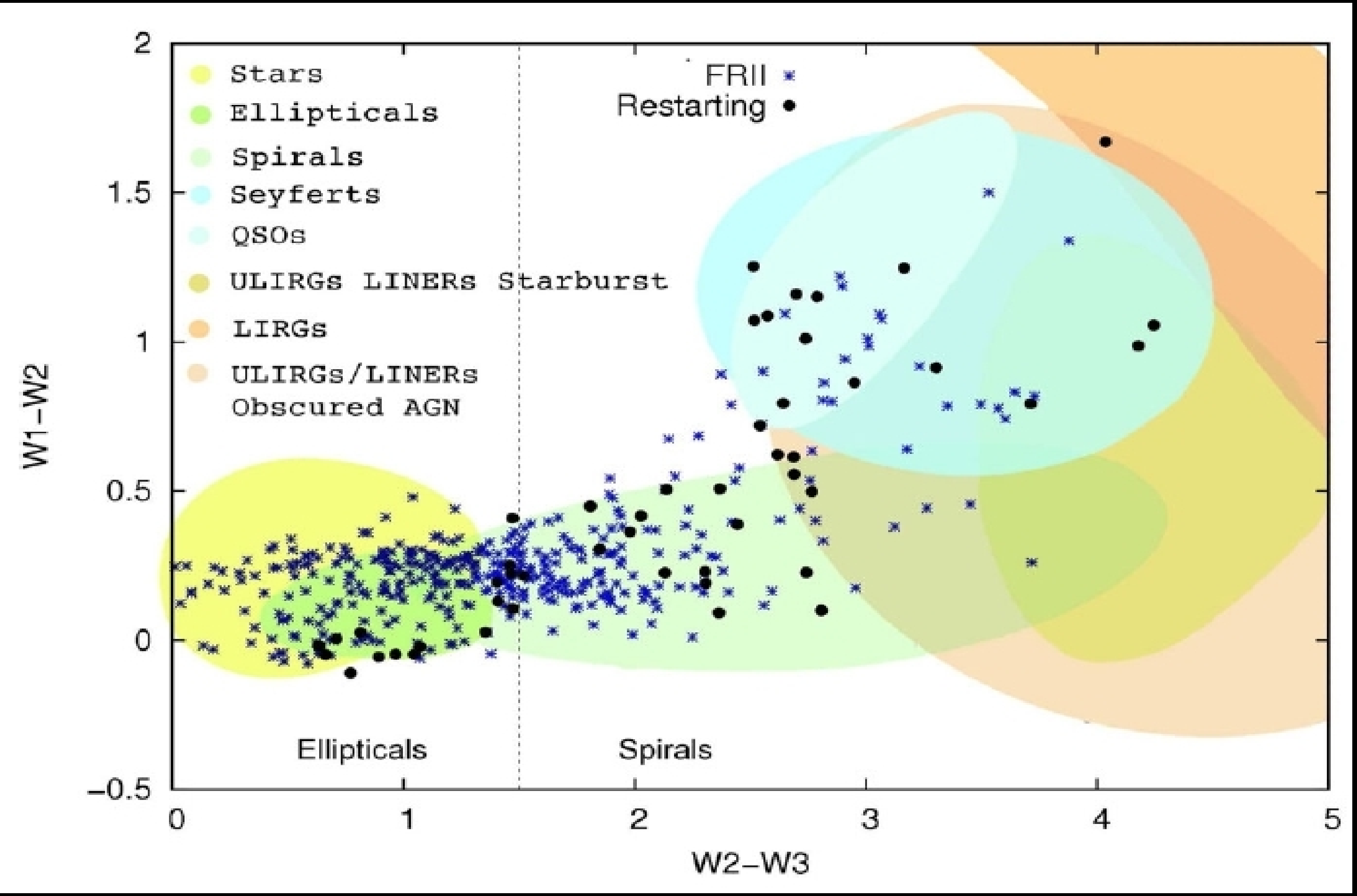

The infrared WISE colour–colour diagram shows that the 67% hosts of recurrent jet activity radio galaxies reside in the region typical for spiral galaxies or other dusty, late-type galaxies with some ongoing star formation

The hosts of restarting radio sources contain a larger amount of young stars.

J1706+4340

Marecki et al. 2016, MNRAS, 463, 338

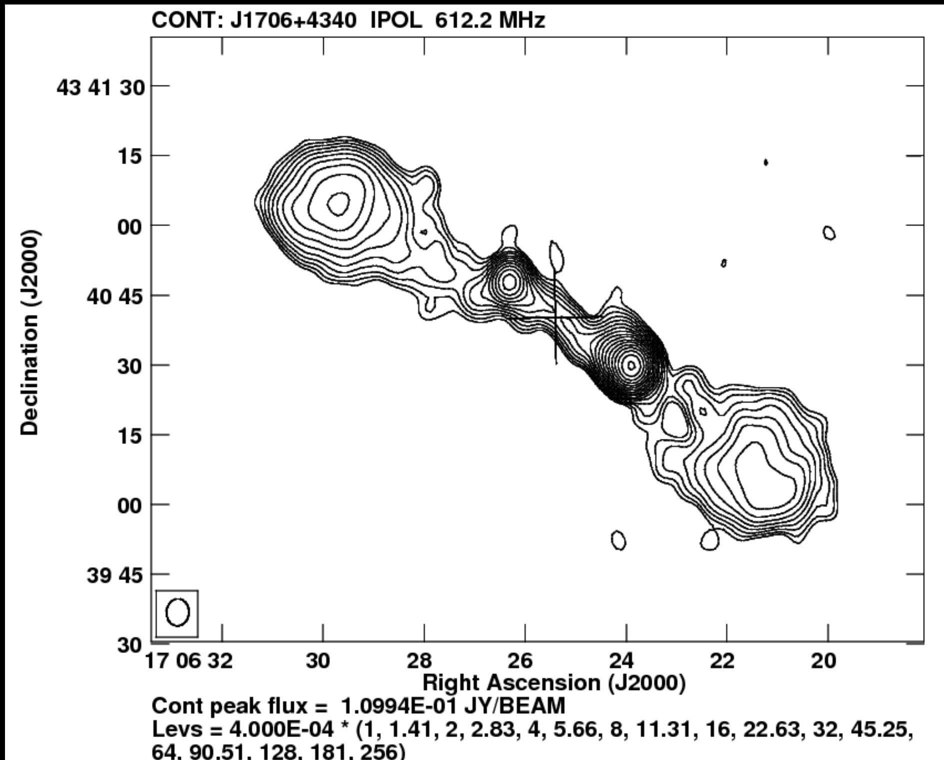

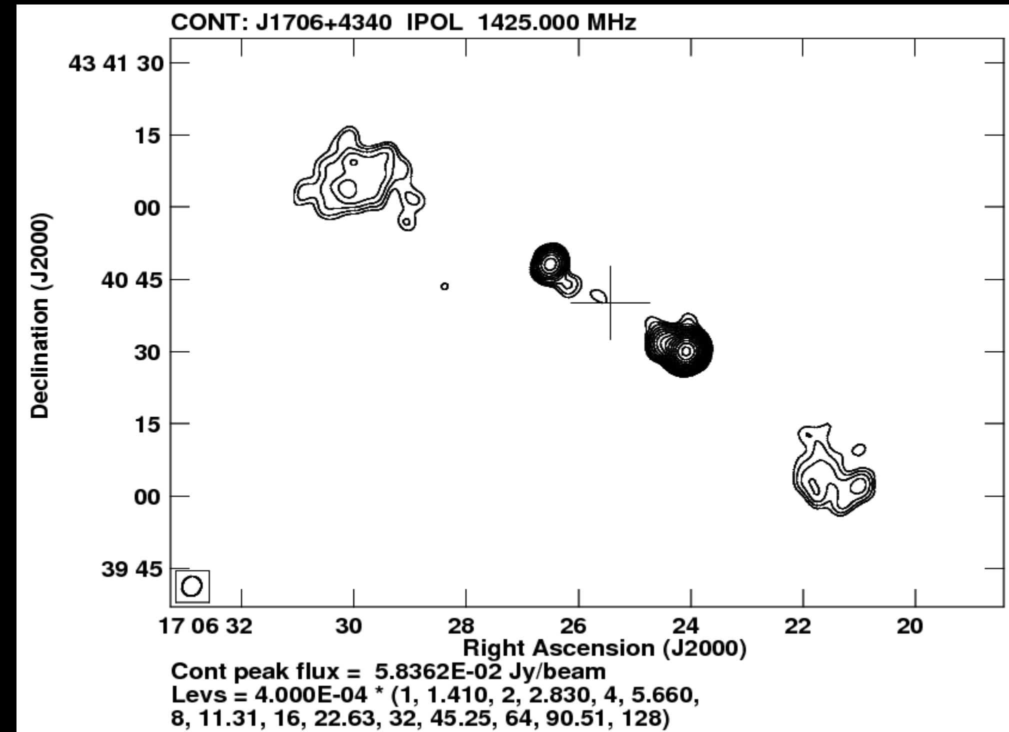

- age:
  of the large-scale outer lobes is in the range 260-300 Myr
  of the inner lobes 12 Myr

- quiesence period about 27 Myr

- injection spectral indices and the jet powers for the inner and the outer doubles are very similar.

=> the spin of the supermassive black hole rather than e.g. an instability of the accretion disc is likely responsible for the jet production and its properties.

4C29.47 (Condon & Mitchell 1984)

Precession of the SMBH spin

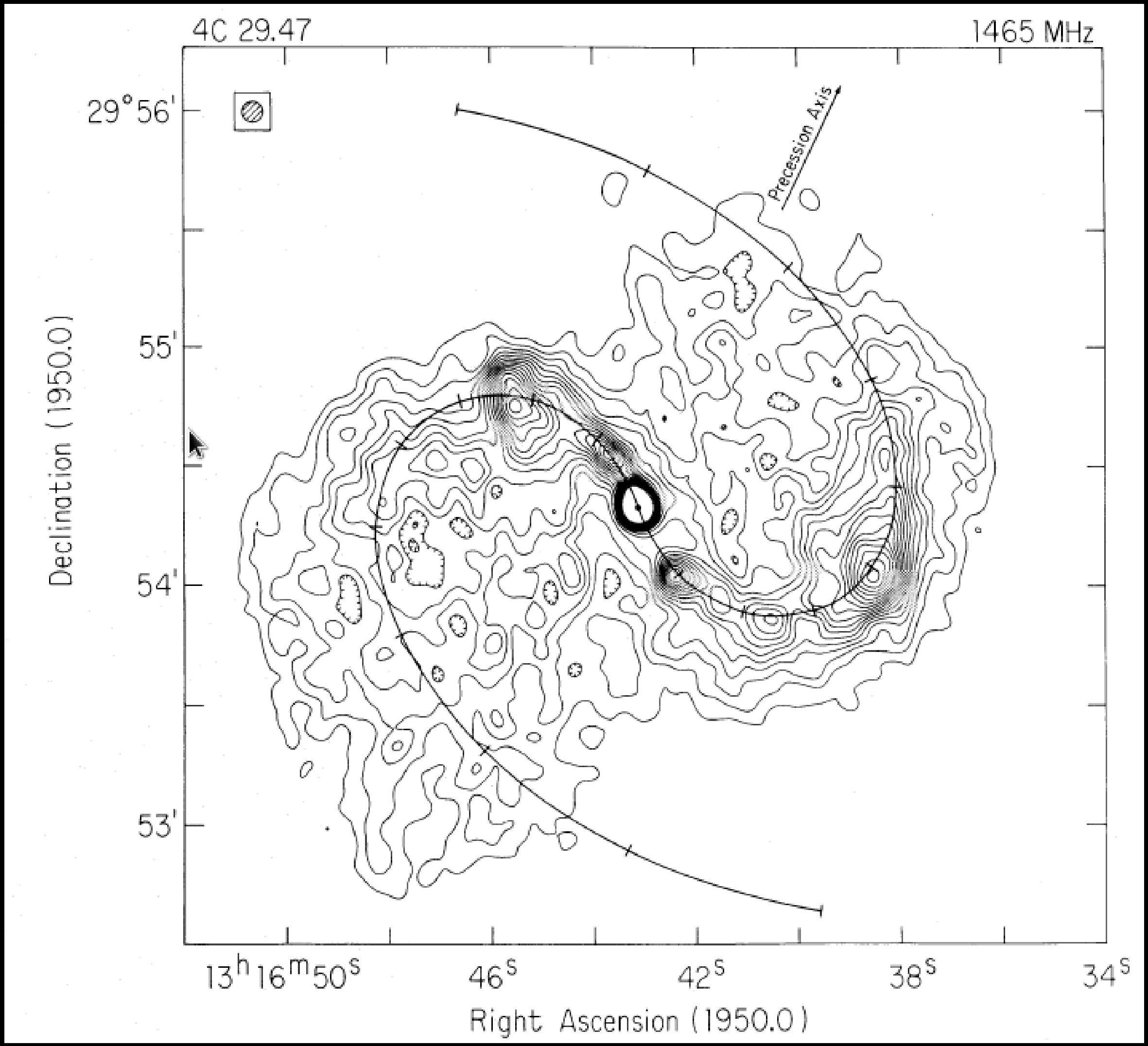

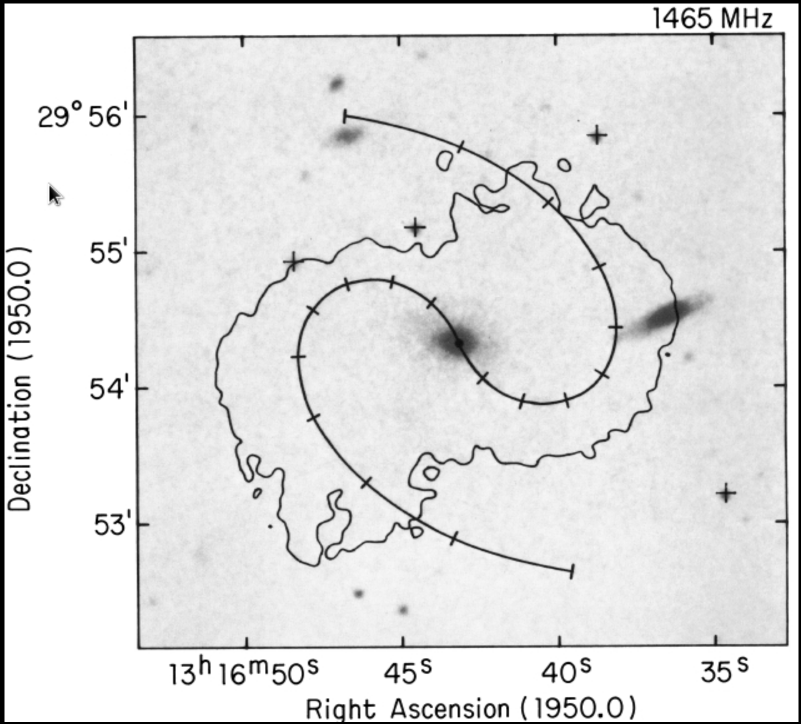

Precession period $6x10^6$ yrs (Lu & Zhou 2005)

Machalski et al. 2016, A&A, 595, 46

3C293

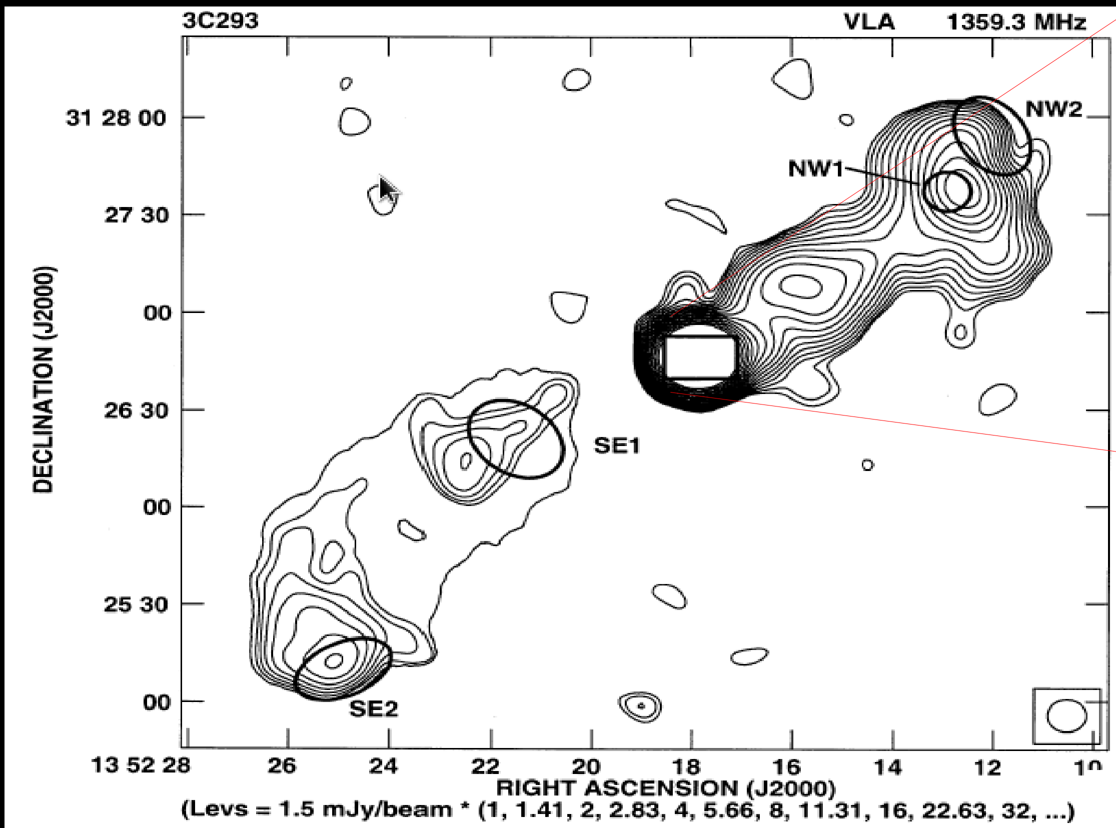

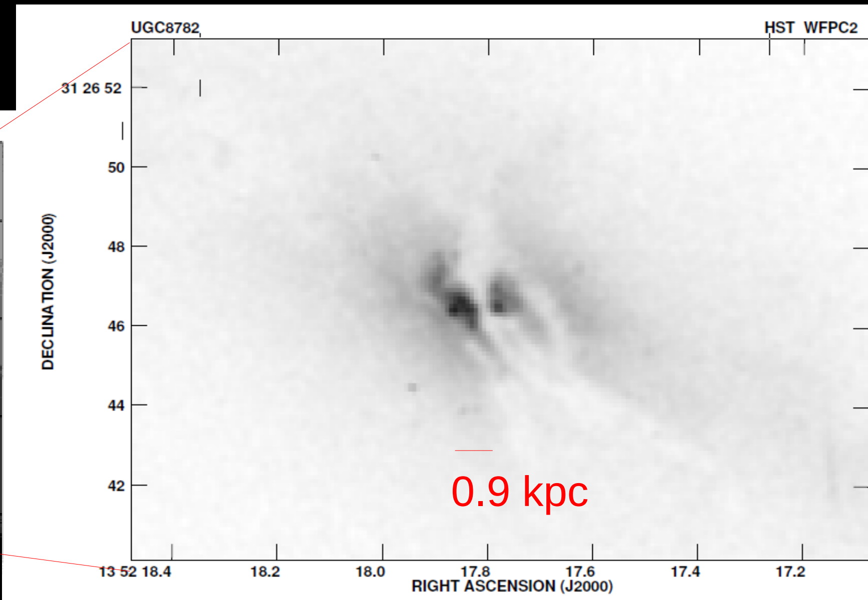

UGC8782

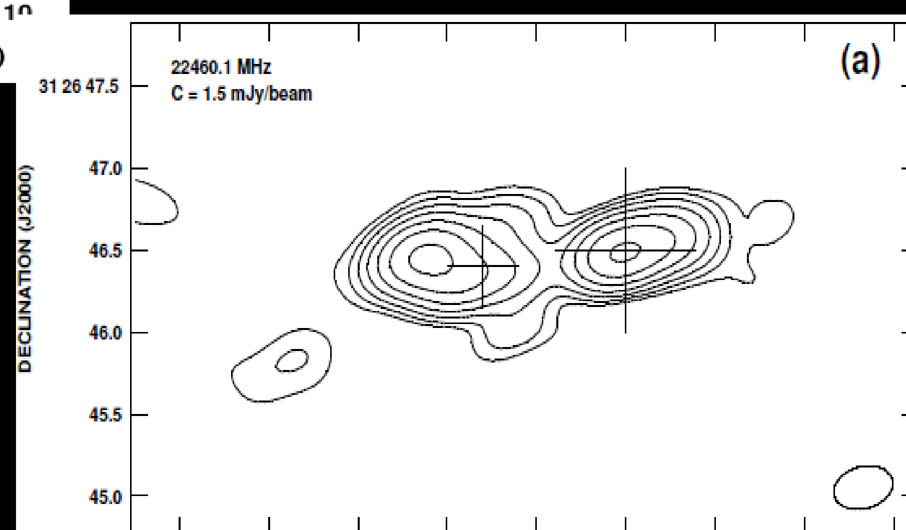

z = 0.0452

size

outer 240 kpc

inner 4 kpc

inclination 40^{o} (X-shape structure)

M_{BH} ~1.6*10^{8} M_{SUN}

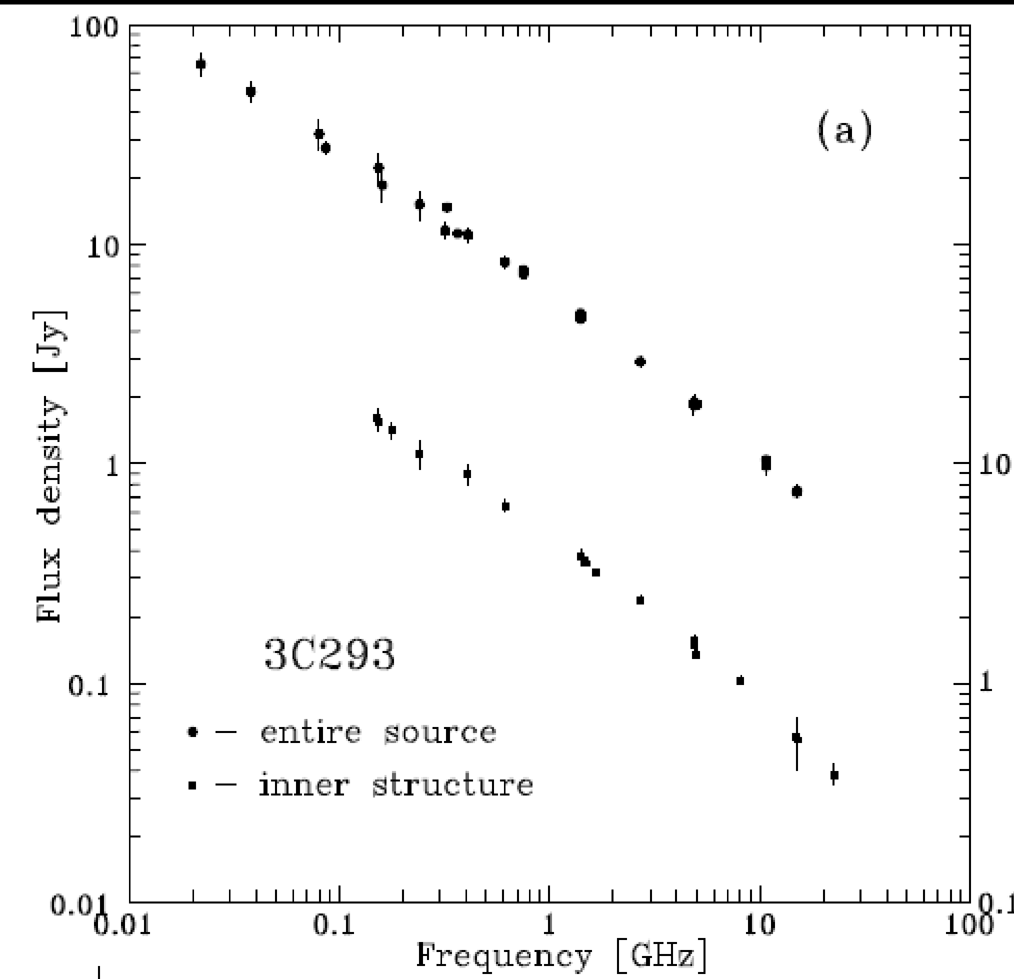

outer lobes ~60 Myr

inner lobes ~0.3 Myr

quiesence period about 1 Myr

=>

- a rapid realignment of the jet axis in 3C293
- the total jet kinetic power, $Q_j \sim 2\mathrm{x}10^{36}$ W, did not change after the realignment episode
- the accretion rate is relatively high, $\dot{M}_{acc}/\dot{M}_{Edd} \sim 0.1$
- relatively low value of the black hole spin, a ~ 0.2

$$\frac{\tau_{\rm align}}{\rm Myr} \sim 0.3 \left(\frac{a}{0.1}\right)^{11/16} \left(\frac{\alpha_{\rm disk}}{0.03}\right)^{13/8} \left(\frac{M_{\rm BH}}{10^8\ M_\odot}\right)^{-1/16} \left(\frac{\dot{M}_{\rm acc}}{0.1\dot{M}_{\rm Edd}}\right)^{-7/8}$$

===> Tilted accretion disk + low value of black hole spin => rapid realignment of the jet axis, leading to the formation of winged radio morphologies <= the Lense-Thirring precession model

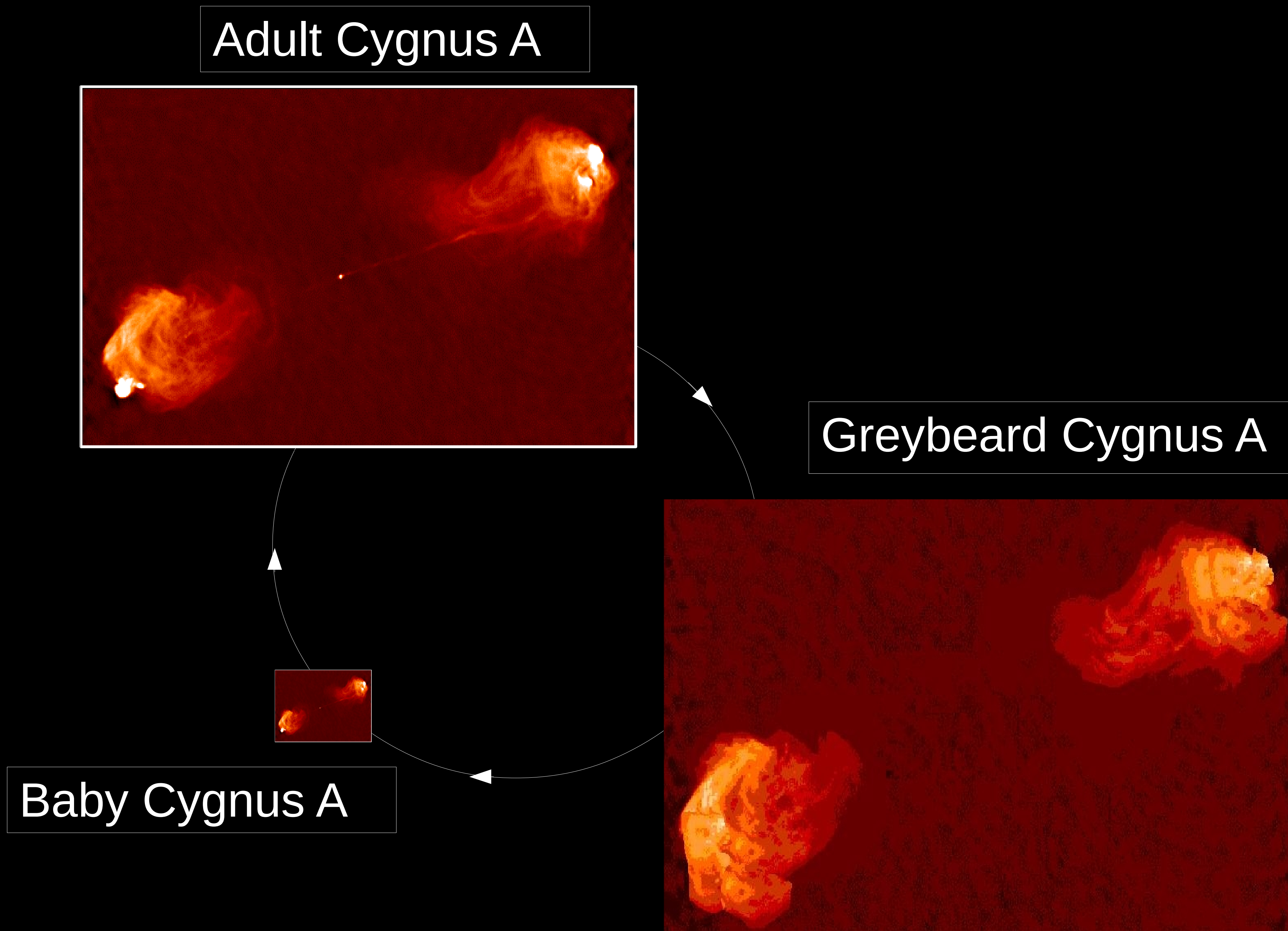
Adult Cygnus A
Greybeard Cygnus A
Baby Cygnus A

Thank you